

Domain Generalization of Pathological Image Segmentation by Patch-Level and WSI-Level Contrastive Learning

Yuki Shigeyasu
Kyushu Univ.
Fukuoka, Japan

Shota Harada
Kyushu Univ.
Fukuoka, Japan

Akihiko Yoshizawa
Nara Medical Univ.
Nara, Japan

Kazuhiro Terada
Kyoto Univ. Hosp.
Kyoto, Japan

Naoki Nakazima
Kyoto Univ. Hosp.
Kyoto, Japan

Mariyo Kurata
Kyoto Univ. Hosp.
Kyoto, Japan

Hiroyuki Abe
The Univ. of Tokyo Hosp.
Tokyo, Japan

Tetsuo Ushiku
The Univ. of Tokyo Hosp.
Tokyo, Japan

Ryoma Bise
Kyushu Univ.
Fukuoka, Japan
bise@ait.kyushu-u.ac.jp

Abstract

In this paper, we address domain shifts in pathological images by focusing on shifts within whole slide images (WSIs), such as patient characteristics and tissue thickness, rather than shifts between hospitals. Traditional approaches rely on multi-hospital data, but data collection challenges often make this impractical. Therefore, the proposed domain generalization method captures and leverages intra-hospital domain shifts by clustering WSI-level features from non-tumor regions and treating these clusters as domains. To mitigate domain shift, we apply contrastive learning to reduce feature gaps between WSI pairs from different clusters. The proposed method introduces a two-stage contrastive learning approach WSI-level and patch-level contrastive learning to minimize these gaps effectively.¹

1 Introduction

Domain shift occurs when training and test datasets have different distributions, leading to performance degradation. In recent years, with the advancement of machine learning, particularly deep learning, various challenges in the field of computer vision have been addressed using machine learning models. These methods are often designed assuming that the training and test datasets share the same distribution. However, this assumption may not hold in real-world scenarios. For instance, in pathology imaging, a model trained on data from one hospital may struggle with data from another hospital. Thus, domain shift remains a critical issue in practical applications [1].

To address domain shift problems, domain generalization has been studied. In traditional domain generalization methods, the model is trained to learn domain-independent feature representations using data labeled with multiple domains. In methods for pathology images, datasets collected from different hospitals typically exhibit domain shifts and are thus treated as separate domains. However, gathering data from multiple hospitals can be challenging due to issues such as privacy concerns and the need to comply with regulations like patient confidentiality. This setting corresponds to single-source domain generalization, where only one labeled domain is available and the model is expected to generalize to unknown domains without any additional supervision.

To avoid the challenges of data collection, we focus on the fact that domain shift may occur not only between different hospitals but also within a single hospital, due to various factors affecting whole slide images (WSIs), such as staining reagents, imaging devices, and tissue thickness or size. These factors are not always consistent within a single hospital, as the characteristics of cells can vary from patient to patient. Therefore, domain shift may occur even within a single hospital. Moreover, domain shifts do not occur within a single WSI, but rather between different WSIs. Within the same WSI, however, the manner in which the domain shift appears (i.e., how feature distributions shift) tends to follow a similar pattern.

In this study, we propose a single-source domain generalization method to address differences in image features caused by domain shifts in pathological images, using data collected from a single hospital. The key contributions are the joint learning of patch-level and WSI-level (patient-level) contrastive learning, as well as the creation of effective WSI and patch pairs,

¹The original paper has been accepted in MVA2025. ©2025 IEICE. Personal use of this material is permitted. Permission from IEICE must be obtained for all other uses.

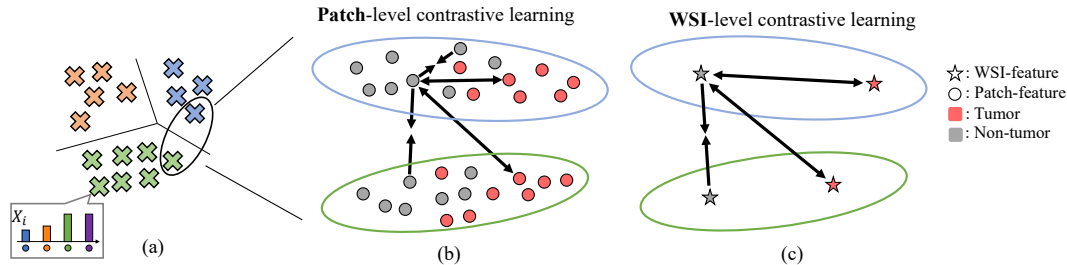


Figure 1. Overview of contrastive learning. (a) WSI clustering result for pseudo domain construction, (b) Patch-level contrastive learning, (c) WSI-level contrastive learning with class-specific prototypes.

which address the challenges posed by the large size and complex tissue structures of WSIs. We evaluate the effectiveness of the proposed method in handling domain shifts caused by hospitals not used in training, based on experiments conducted with real clinical data.

2 Related Work

Domain generalization: Domain generalization learns domain-independent feature representations using only source data from multiple domains, aiming to improve classification on unknown target domains. Representative domain generalization methods include contrastive learning [2], adversarial learning [3, 4], meta-learning [5, 6], and data augmentation [7, 8]. However, these methods typically require multi-domain datasets, making them impractical for pathology image segmentation, where acquiring data from multiple hospitals is challenging.

Single-source domain generalization: Single-source domain generalization method improves classification performance on unknown target domains using a single domain for training. Additionally, since it typically ignores domain labels, it can also handle multiple source domains. Representative approaches include adversarial learning-based methods for data augmentation, which increase the diversity of the source domain [9, 10, 11], methods that remove features strongly dependent on the domain [12], and methods that adapt to test data during testing [13]. Unlike these methods, in this study, we propose a domain generalization approach that addresses domain shift even within the same hospital, which is traditionally considered a single domain. We aim to resolve this domain shift by performing contrastive learning using WSI features.

Contrastive learning: Contrastive learning trains models to bring similar data points closer and push dissimilar ones in the feature space. It is commonly used in self-supervised learning, where augmented data is treated as similar data, and all other data are considered dissimilar. Representative methods include SimCLR [14], which demonstrates improvements in accuracy through various data augmentation strategies, the use of a two-layer MLP, and increasing batch sizes. In

supervised contrastive learning [15], same-class data are treated as similar and data from different classes as dissimilar. Our method follows this approach, applying contrastive learning accordingly.

3 Proposed Method

Our method performs domain generalization through the joint learning of patch-level and WSI-level contrastive learning, as shown in Fig. 1. To effectively create pairs of WSI features for contrastive learning, our method extracts the WSI features using the Bag of Visual Words (BoVW) approach, followed by clustering, as shown in Fig. 2. Based on the clusters, WSI features from different groups are used to form negative pairs, and those from the same group are used to form positive pairs.

3.1 Problem setting

Let us assume that a set of M source WSIs $\{\mathbf{X}_i, \mathbf{S}_i\}_{i=1}^M$ is given as the training data. Here, \mathbf{X} represents the original WSI, and \mathbf{S} is the ground truth segmentation mask. Since each WSI \mathbf{X}_i is of very high resolution, directly inputting it into the model is difficult. Following existing studies [16, 17], we handle the WSI segmentation task by dividing the WSI into patches, thereby converting the segmentation task into a classification task for patch images. Let the set of L patch images from the source data be represented as $\mathcal{D} = \{\mathbf{x}_j, y_j, id\}_{j=1}^L$. Here, $\mathbf{x}_j \in \mathbf{X}_{id}$ denotes a patch image cut from the WSI, id is the index of the WSI, and $y_j \in \{0, 1\}$ represents the class label, where 0 corresponds to non-tumor and 1 corresponds to tumor. In this task, given \mathcal{D} , the model is trained through domain generalization so that the trained model performs effectively on data from hospitals not used during training.

3.2 Grouping WSIs using BoVW

Domain shift in WSIs arises from factors like staining reagents, tissue thickness, and patient characteristics, affecting entire WSIs rather than individual cells. Thus, a common domain shift is assumed within each

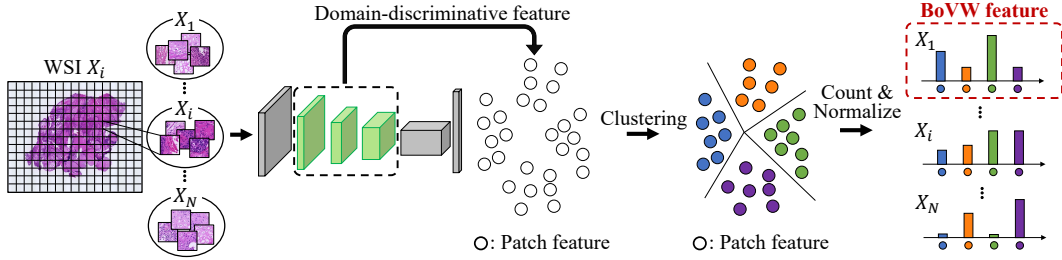


Figure 2. Grouping of WSIs

WSI. To address this, we group WSIs using BoVW-like strategy, treating each group as a pseudo-domain, and contrastive learning is then employed to reduce inter-domain differences. Clustering is performed using domain-discriminative features—independent of class-related characteristics—to facilitate effective domain generalization [18].

Fig. 2 shows the WSI grouping method. Global features can be biased by cancer type ratios or tumor region proportions, while BoVW better preserves local feature distributions relevant to staining-related domain shifts. For instance, WSIs with different tumor region ratios may have dissimilar global features despite similar patch-level features.

To mitigate this, we focus on the non-tumor regions for feature extraction. We assume that factors affecting domain shift, such as staining reagents, imaging devices, and tissue thickness or size, are consistent within a WSI, meaning that the direction of shift across different patch images within a WSI is similar. Additionally, the appearance of non-tumor regions is more consistent than that of tumor regions. Therefore, we use non-tumor regions, which can better represent the domain shift of a WSI, for feature extraction.

We extract WSI features using the BoVW algorithm. Domain-discriminative features [18] from “non-tumor” patches are clustered via K-means. For each WSI, we count the number of patch features per cluster, normalize them, and use the result as a BoVW feature vector. This vector captures the distribution of “non-tumor” features. A larger distance between two such vectors indicates a greater domain shift.

To make pairs for contrastive learning, we perform clustering to the distribution of BoVW WSI features using K-means method. The resulting clusters represent the groups, and when performing contrastive learning, pairs are created between data from different groups. This approach is expected to create efficient pairs for learning.

3.3 WSI-based contrastive learning

Using the above method, we construct pairs and perform contrastive learning based on WSI features. While typical domain generalization mitigates patch-level shifts, WSI-level shifts are more dominant in our

setting. Therefore, we apply contrastive learning at both the patch and WSI levels to effectively address domain shift on both local and global level.

WSI-level contrastive learning: To address domain shifts across WSIs, we apply WSI-level contrastive learning. Using BoVW features, we randomly sample feature pairs from different clusters—representing large domain shifts—and bring them closer. For representation learning, we use class prototypes $\mathbf{c} \in \mathcal{C}$, which are mean features for each class (non-tumor and tumor), as shown in Fig. 1(c). Contrastive learning pulls same-class WSI features (positive pairs) closer and pushes different-class features (negative pairs) apart. Fig. 1(c) shows an example where the non-tumor feature of the top WSI is used as the anchor.

Let the set of features for positive pairs in the source dataset \mathcal{D} be denoted as $P_w(\mathbf{c}, \mathcal{C})$, and the set of features for negative pairs as $N_w(\mathbf{c}, \mathcal{C})$. The loss function for WSI-level contrastive learning between WSIs denoted as L_w is as follows:

$$L_w = \sum_{\mathbf{c}_j \in \mathcal{C}} \frac{-1}{|P(\mathbf{c}_j, \mathcal{C})|} \sum_{\mathbf{c}^+ \in P_w(\mathbf{c}_j, \mathcal{C})} \log \frac{S(\mathbf{c}_j, \mathbf{c}^+)}{S(\mathbf{c}_j, \mathbf{c}^+) + \sum_{\mathbf{c}^- \in N_w(\mathbf{c}_j, \mathcal{C})} S(\mathbf{c}_j, \mathbf{c}^-)}, \quad (1)$$

where \mathbf{c}_j is an anchor, \mathbf{c}^+ , \mathbf{c}^- are positive and negative samples.

This approach encourages patches belonging to the same WSI to move in the same direction, thus bringing the distributions of the same class closer together and pushing the distributions of different classes further apart.

Patch-level contrastive learning: To align the patch-level features between WSIs, patch-level contrastive learning is performed. Specifically, in patch-level contrastive learning, we select patch-level positive and negative pairs from the WSI-level pairs that are used for WSI-level contrastive learning. The anchor refers to the reference data, the positive example refers to data from the same class as the anchor, and the negative example refers to data from a different class than the anchor, as shown in Figure 1 (b).

Let the patch-level feature vector \mathbf{v} of anchor \mathbf{x} be represented as $f(\mathbf{x}) = \mathbf{v} \in \mathcal{V}$, where f is the feature extractor. Furthermore, let the set of features for positive pairs in the source dataset \mathcal{D} be denoted by $P_p(\mathbf{v}, \mathcal{V})$,

the set of features for negative pairs by $N_p(\mathbf{v}, \mathcal{V})$, and the similarity between feature vectors \mathbf{v}_1 and \mathbf{v}_2 be computed using a temperature parameter τ . The loss function for patch-level contrastive learning between patches, denoted as L_p , is as follows:

$$L_p = \sum_{\mathbf{v}_j \in \mathcal{V}} \frac{-1}{|P(\mathbf{v}_j, \mathcal{V})|} \sum_{\substack{\mathbf{v}^+ \in \\ P_p(\mathbf{v}_j, \mathcal{V})}} \log \frac{S(\mathbf{v}_j, \mathbf{v}^+)}{S(\mathbf{v}_j, \mathbf{v}^+) + \sum_{\substack{\mathbf{v}^- \in \\ N_p(\mathbf{v}_j, \mathcal{V})}} S(\mathbf{v}_j, \mathbf{v}^-)} \quad (2)$$

where \mathbf{v}_j is an anchor, \mathbf{v}^+ , \mathbf{v}^- are patch-level positive and negative samples.

In addition to the contrastive learning loss functions for patches and WSIs, L_p and L_w , the cross-entropy loss L_c is also used to train the fully connected layer. The overall loss is defined as $L_w + L_p + L_c$.

4 Experiments

We evaluated the proposed method in a two-class (non-tumor, tumor) segmentation task using whole-slide images (WSIs) of cervix tissues. The source data, collected from Kyoto University Hospital, was used for training, while target data, collected from a different hospital (The University of Tokyo Hospital), was used for testing.

For the evaluation of segmentation performance, we used commonly employed metrics in segmentation tasks: precision, recall, F1 score, and macro-F1 score. Here, precision, recall, and F1 score treat the tumor class as positive, while macro-F1 represents the average F1 score, considering both the tumor and non-tumor classes as positive.

Dataset: Cervical cancer tissue slices were stained with Hematoxylin and Eosin (H&E) and scanned using a virtual slide scanner at $40\times$ magnification. The source dataset consists of 300 WSIs, and the target dataset includes 108 WSIs. For the experiments, 236 WSIs from the source were used for training, 64 for validation, and all target WSIs for testing. After splitting, 256×256 patches were extracted at $40\times$ magnification. Only patches whose ground-truth masks were entirely composed of a single class were used for training as that class. The source dataset yielded 356,079 patches in total—28,371 tumor and 327,708 non-tumor—while the target dataset contained 68,164 patches—6,071 tumor and 62,093 non-tumor.

Implementation details: For feature extraction, we used a modified version of ResNet-18 [19] pretrained on ImageNet, replacing the final layer with a two-layer MLP. Training was performed using SGD with a learning rate of 10^{-5} and a batch size of 128. From each of the two WSIs, 32 patches were randomly sampled for both tumor and non-tumor classes. If a WSI had fewer than 32 patches for a class, oversampling was applied.

Performance evaluation: We compared segmentation performance across four methods: 1) a baseline method that uses only the cross-entropy loss for training on the source data, 2) a method that leverages

Table 1. Comparison of segmentation performance and ablation study.

Method	precision	recall	F1	macro-F1
Baseline	0.4255	0.7218	0.5354	0.7360
w/ contrastive	0.4457	0.6697	0.5344	0.7380
MMLD [18]	0.4215	0.7457	0.5385	0.7368
L2D [20]	0.5090	0.5586	0.5326	0.7427
Ours	0.4827	0.7521	0.5880	0.7675

style features to create domain-discriminative representations and assigns domain labels based on latent domains of the images through clustering for domain generalization [18] (MMLD), 3) a method that extracts style features using mutual information and performs domain generalization [20] (L2D), and 4) the proposed method (Ours). In both MMLD and the proposed method, K-means clustering was used to assign domain labels, and the value of K was varied as 2, 4, 6, 8, and 10. The value that yielded the highest performance on the validation set was used for comparison.

Table 1 shows the performance results for each method. Existing domain generalization methods show improvements in accuracy on several metrics compared to the Baseline. The proposed method, which performs domain generalization using WSI features, outperforms the Baseline on all metrics and achieves the highest F1 and macro-F1 scores, further improving performance compared to other domain generalization methods.

Table 1 also presents the results of the Ablation study. Baseline+contrastive (w/ contrastive) applies contrastive learning by using cross-entropy loss on source data, treating same-class patches as positive and different classes as negative. Compared to the simple cross-entropy loss (Baseline), Baseline+contrastive shows limited improvement in performance. However, the proposed method (Ours) improves performance across all metrics. This suggests that the performance improvement of the proposed method is not solely attributed to the introduction of general contrastive learning.

5 Conclusion

In this paper, we proposed a method to address domain shift in pathology images, caused by factors such as tissue thickness and staining variations. Assuming that domain shift occurs at the whole-slide image (WSI) level, we introduced a contrastive learning approach that operates not only at the patch level but also at the WSI level using average patch features. Our method effectively reduces domain shift and outperforms existing domain generalization techniques, achieving state-of-the-art segmentation performance under realistic domain shift conditions without requiring multi-domain training data.

Acknowledgement This study is supported by Grant-in-Aid for Challenging Research (Exploratory) JP23K18509, Cross-ministerial Strategic Innovation Promotion Program (SIP) on “Integrated Health Care

System” Grant Number JPJ012425, and JST ASPIRE Program Japan Grant Number JPMJAP2403.

References

- [1] K. Muandet *et al.*, “Domain generalization via invariant feature representation,” in *ICML*, vol. 28, 2013, pp. 10–18.
- [2] C. Yoon *et al.*, “Generalizable feature learning in the presence of data bias and domain class imbalance with application to skin lesion classification,” in *MICCAI*, 2019, pp. 365–373.
- [3] H. Li *et al.*, “Domain generalization with adversarial feature learning,” in *CVPR*, 2018.
- [4] K. Akuzawa *et al.*, “Adversarial invariant feature learning with accuracy constraint for domain generalization,” in *ECML PKDD*, 2020, pp. 315–331.
- [5] D. Li *et al.*, “Learning to generalize: Meta-learning for domain generalization,” *AAAI*, vol. 32, no. 1, 2018.
- [6] Y. Zhao *et al.*, “Learning to generalize unseen domains via memory-based multi-source meta-learning for person re-identification,” in *CVPR*, 2021, pp. 6277–6286.
- [7] K. Zhou *et al.*, “Semi-supervised domain generalization with stochastic stylematch,” *Int. J. Comput. Vis.*, pp. 1–11, 2023.
- [8] F. Borlino *et al.*, “Rethinking domain generalization baselines,” in *ICPR*, 2021, pp. 9227–9233.
- [9] X. Fan *et al.*, “Adversarially adaptive normalization for single domain generalization,” in *CVPR*, 2021, pp. 8208–8217.
- [10] L. Li *et al.*, “Progressive domain expansion network for single domain generalization,” in *CVPR*, 2021, pp. 224–233.
- [11] Z. Wang *et al.*, “Learning to diversify for single domain generalization,” in *ICCV*, 2021, pp. 834–843.
- [12] Z. Huang *et al.*, “Self-challenging improves cross-domain generalization,” in *ECCV*, 2020, pp. 124–140.
- [13] Q. Liu *et al.*, “Single-domain generalization in medical image segmentation via test-time adaptation from shape dictionary,” *AAAI*, vol. 36, no. 2, pp. 1756–1764, 2022.
- [14] T. Chen *et al.*, “A simple framework for contrastive learning of visual representations,” in *ICML*, 2020.
- [15] P. Khosla *et al.*, “Supervised contrastive learning,” *NeurIPS*, 2020.
- [16] H. Tokunaga *et al.*, “Adaptive weighting multi-field-of-view cnn for semantic segmentation in pathology,” in *CVPR*, 2019.
- [17] H. Li *et al.*, “Task-specific fine-tuning via variational information bottleneck for weakly-supervised pathology whole slide image classification,” in *CVPR*, 2023, pp. 7454–7463.
- [18] T. Matsuura and T. Harada, “Domain generalization using a mixture of multiple latent domains,” *AAAI*, vol. 34, no. 07, pp. 11 749–11 756, 2020.
- [19] K. He *et al.*, “Deep residual learning for image recognition,” in *CVPR*, 2016.
- [20] Z. Wang *et al.*, “Learning to diversify for single domain generalization,” in *ICCV*, 2021, pp. 834–843.